www.czasopisma.pan.pl PAN POLSKA AKADEMIA NAUK www.journals.pan.pl

Arch. Metall. Mater. **63** (2018), 3, 1459-1462

DOI: 10.24425/123828

Y.-A. JOO*, T.-S. YOON**, S.-H. PARK***, K.-A. LEE*#

# MICROSTRUCTURE AND COMPRESSION PROPERTIES OF Fe-Cr-B ALLOY MANUFACTURED USING LASER METAL DEPOSITION

Fe-Cr-B alloy is a material with precipitation of boride inside Fe matrix, and it features outstanding hardness and wear resistance properties. However, Fe-Cr-B alloy is a difficult material to process, making it difficult to use as a bulk type structure material which requires delicate shapes. This study attempted to manufacture Fe-Cr-B alloy using a 3D printing process, laser metal deposition. This study also investigated the microstructure, hardness and compression properties of the manufactured alloy. Phase analysis results is confirmed that $\alpha$-Fe phase as matrix and $(Cr, Fe)_2B$ phase as reinforcement phase. In the case of $(Cr, Fe)_2B$ phase, differences were observed according to the sample location. While long, coarse, unidirectional needle-type boride phases (~11 μm thickness) were observed in the center area of the sample, relatively finer boride phases (~6 μm thickness) in random directions were observed in other areas. At room temperature compression test results confirmed that the sample had a compression strength is approximately 2.1 GPa, proving that the sample is a material with extremely high strength. Observation of the compression fracture surface identified intergranular fractures in areas with needle-type boride, and transgranular fractures in areas with random borides. Based on this results, this study also reviewed the deformation behavior of LMD Fe-Cr-B alloy in relation to its microstructures.

*Keywords:* Fe-Cr-B composite, Laser Metal Deposition, Bulk type, Microstructure, Compressive properties

## 1. Introduction

Fe-Cr-B based alloy is a material in which a boride phase with high hardness is precipitated in the Fe-matrix [1]. Fe-Cr-B based alloy is characterized by its advantages of excellent wear resistance properties and high hardness. Due to such, it is manufactured as hardfacing of heavy equipment parts used in excavating and mining industries through spraying or welding processes [2]. However, Fe-Cr-B-based alloy is a difficult in plastic processing material, and it is difficult to fabricate a bulk type structural material with elaborate shapes.

Laser Metal Deposition (LMD) is a process that laminates powder layer by layer by forming a molten pool on the target material surface [3]. LMD is able to partially repair expensive parts at an affordable price, and it is also able to manufacture 3D shaped parts easily. Due to such advantages, LMD is commonly used in various fields such as aerospace and automobiles, and the number of applicable fields is expected to grow [4].

Currently, Fe-Cr-B based alloy is commonly manufactured using spraying and welding processes such as plasma transferred arc (PTA), high velocity oxygen fuel (HVOF) and high energy electron beam irradiation (HEEBI) to be used as coating materials, and there are many studies reporting on such [5-7]. In some studies, Fe-Cr-B based alloy is manufactured as a bulk type using casting and metal injection molding (MIM), and their microstructural, corrosion and wear properties were reported [8,9]. At present, there are no studies that have looked into bulk type Fe-Cr-B-based alloy manufactured using 3D printing.

This study manufactured a bulk type Fe-Cr-B-based alloy using LMD process and investigated its initial microstructure, hardness and room temperature compression properties. Also, the surface and cross-section of the compressive specimen were analyzed to determine the relationship between the deformation behavior and microstructure of the LMDed Fe-Cr-B-based alloy.

## 2. Experimental

The powder feedstock used in this study was “M” powder by Armacor, which has an alloy composition of Fe-43Cr-5.6B-1.8Si-0.2S-0.17C(wt.%). Fig. 1a,b show the shape of M powder, which is a clean, spherical shape, and the size ($D_{50}$) measured 35.1 μm on average. The process parameters applied to manufacture a bulk type Fe-Cr-B-based alloy using LMD are listed in Table 1, and the specimen in Fig. 1c was obtained.

To observe the initial microstructure of the LMDed Fe-Cr-B-based alloy, the specimen underwent mirror polishing up to 1 μm using SiC sandpaper. A scanning electron microscope

* INHA UNIVERSITY, DEPARTMENT OF MATERIALS SCIENCE AND ENGINEERING, INCHEON 22212, REPUBLIC OF KOREA
** BESTNER, EUMSEONG-GUN 15244, REPUBLIC OF KOREA
*** RIST, POHANG-SI, GYEONGBUK 37673, REPUBLIC OF KOREA
# Corresponding author: keeahn@inha.ac.kr

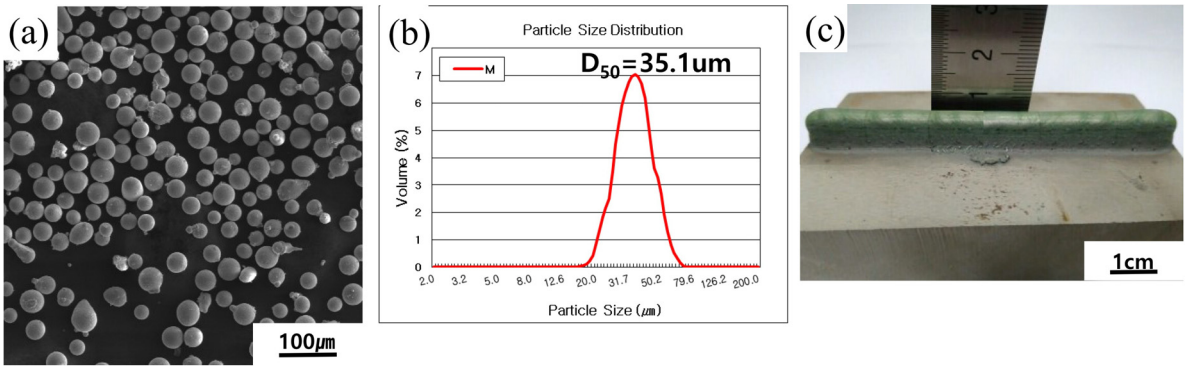


Fig. 1. (a) Morphology of the Fe-Cr-B powder particle, (b) particle size distribution and (c) laser metal deposited sample

TABLE 1

Process conditions of the Fe-Cr-B alloy manufactured by laser metal deposition process

| Process parameter | Conditions |
|---|---|
| Laser Power(kW) | 2 |
| Scanning Speed(mm/s) | 30 |
| Powder Flow Rate (rpm) | 1 |

(SEM, Tescan, VEGA II LMU), energy dispersive spectroscopy (EDS), X-ray diffraction (XRD, Rigaku KRD Ultima IV) and electron probe X-ray microanalyzer (EPMA, EPMA-1600) were used for microstructural and phase analysis. To measure the phase ratio, 20 measurements were made of the SEM images using an image analyzer, and their average was calculated. A Vickers hardness tester was used to measure Vickers hardness using a 5 Kgf load, and 12 measurements were made to calculate the average.

To investigate the compression property of LMDed Fe-Cr-B-based alloy, three compression tests were performed using MTS 810 at a deformation rate of $10^{-3}$ $sec^{-1}$. The compression specimen was processed to a cylindrical shape measuring 6 mm × 4 mm (H×D). After the compression test, SEM was used to observe the surface and cross section of the compressed specimen to determine the fracture behavior.

## 3. Results and discussion

Fig. 2 shows the XRD phase analysis results of the LMDed Fe-Cr-B based alloy. The XRD phase analysis of the LMDed Fe-Cr-B based alloy confirmed that the specimen is composed of a $\alpha$-Fe and $(Cr, Fe)_2B$ of orthorhombic structure. The boride phase of the $M_2B$ structure was formed by the metal elements Fe and Cr combining with the non-metal element B, and there are reports stating that orthorhombic structure of $(Cr, Fe)_2B$(<0.7 wt.% Fe) or tetragonal structure of $(Fe, Cr)_2B$(>0.75 wt.% Fe) is formed according to the Fe and Cr ratio within the boride phase [10].

Fig. 3 shows the initial microstructure of the LMDed Fe-Cr-B based alloy. Initial microstructural observations (Fig. 3a,b) confirmed that the LMDed Fe-Cr-B based alloy consists of two phases. As a results of the EDS analysis, it was confirmed that a relatively smaller ratio area was the Fe-matrix and the relatively

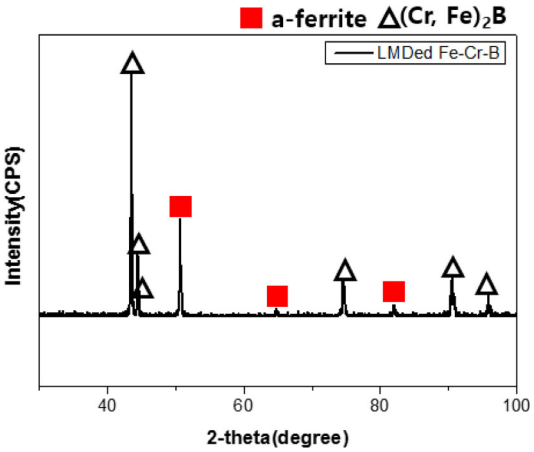


Fig. 2. X-ray diffraction analysis results of Fe-Cr-B alloy fabricated with laser metal deposition

larger ratio area was the $(Fe, Cr)_2B$. Quantitative measurement of microstructural characteristics confirmed that the ratio of Fe-matrix is 30.4%, boride phase is 68.3% and porosity is 1.3%. Such findings classify the specimen as an intrinsic composite which forms a reinforcement phase without artificially adding reinforcements.

Fig. 3a,b show that the boride shape and size varied according to the location on the manufactured specimen. First, long, macro needle type boride phases (thickness up to 11 μm) were formed at the center region of the specimen (Fig. 3a). Meanwhile, randomly distributed boride phases (with thickness up to 6 μm) were formed on the surface region of the specimen. Also, as shown in Fig. 3c, fine boride phases of 1 μm were found in between the main boride phases. The randomly distributed boride phases are suspected to be related to the heat flow direction occurring during solidification [4]. Meanwhile, Fe-Cr-B based alloy is reported to cause a metamorphic transition (crystalline-to-amorphous) in some thermal spray processes [3-5]. However, the specimen manufactured in this study did not cause a metamorphic transition but formed evenly extracted boride phases from the Fe-matrix interior, as shown in Figs. 2,3.

In order to observe the distribution of B element, which cannot be easily detected with EDS analysis, EPMA analysis was performed, and the results are shown in Fig. 4. B element, which is the main element that forms a reinforcement phase, was

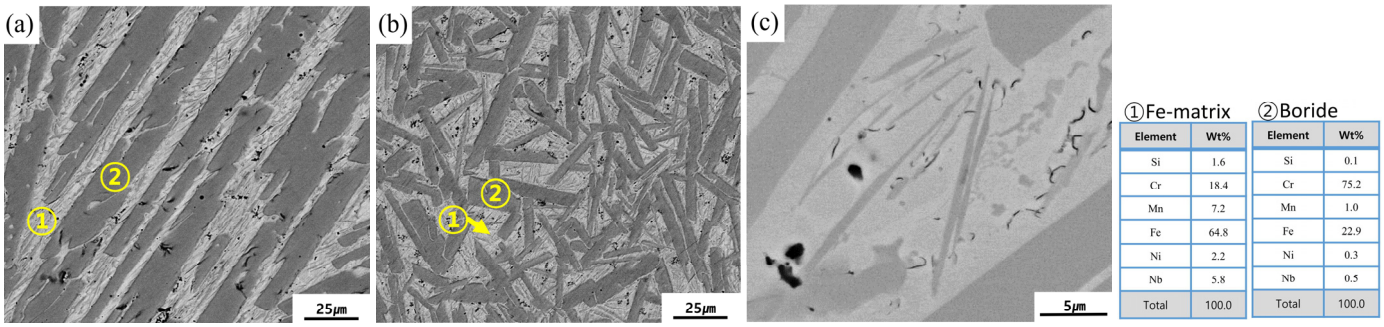


| Element | Wt% |
|---|---|
| Si | 1.6 |
| Cr | 18.4 |
| Mn | 7.2 |
| Fe | 64.8 |
| Ni | 2.2 |
| Nb | 5.8 |
| Total | 100.0 |

| Element | Wt% |
|---|---|
| Si | 0.1 |
| Cr | 75.2 |
| Mn | 1.0 |
| Fe | 22.9 |
| Ni | 0.3 |
| Nb | 0.5 |
| Total | 100.0 |

Fig. 3. SEM/EDS microstructures of (a) middle area (b) surface area and (c) between main borides

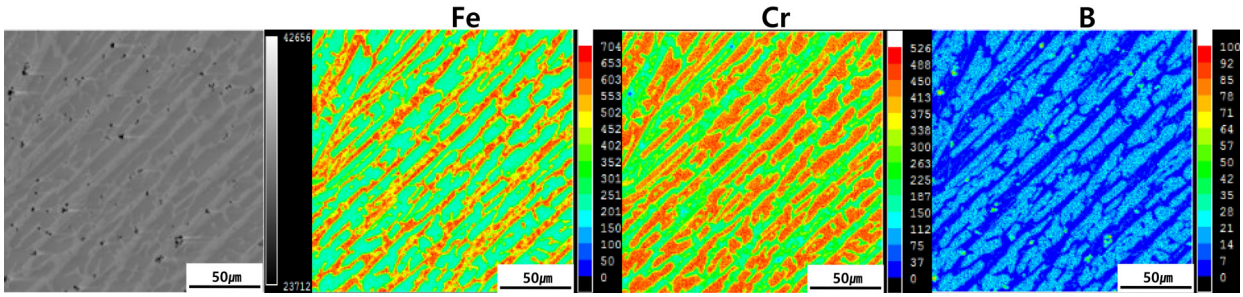


Fig. 4. EPMA analysis results of LMDed Fe-Cr-B alloy

confirmed to be present in $(Cr, Fe)_2B$ phase at high concentration, as shown in Fig. 4. In other words, EPMA analysis confirmed that the Fe-matrix contained a high concentration of Fe and $(Cr, Fe)_2B$ contained a high concentration of B and Cr.

In general, the mechanical properties of a metal matrix composite (MMC) are known to be dependent on the shape, size, distribution and volume fraction of a reinforcement phase. As the LMDed Fe-Cr-B composite used in this study achieved a relatively high $(Cr, Fe)_2B$ ratio distributed evenly throughout the specimen, it is expected that it will achieve outstanding mechanical properties. The hardness of the specimen measured 838.4Hv on average, and the hardness per boride ratio (Hv/vol.%) was 12.3. The hardness per boride ratio of the specimen was compared to the hardness per boride ratio of other Fe-Cr-B based alloys with the same composition manufactured using different processes. The processes compared were the spraying and welding processes commonly applied to Fe-Cr-B based alloys, PTA, HVOF and HEEBI. The hardness per boride ratio of Fe-Cr-B based alloys manufactured using PTA, HVOF and HEEBI were 11.2, 11.9 and 10.3, respectively [5-7]. In other words, the hardness of the LMDed Fe-Cr-B based alloy was relatively greater than Fe-Cr-B based alloys manufactured using thermal spray processes.

Fig. 5 shows the stress-strain curve obtained from the room temperature compression test performed on the specimen. The peak stress measured from the room temperature compression test was an outstanding 2014.7 MPa. The high strength of LMDed Fe-Cr-B based alloy is suspected to be due to the fine reinforcement phases evenly distributed throughout the specimen. In addition, fracturing occurred in the specimen immediately after the yield point on the stress-strain curve. In general, MMCs are reported to not accept plastic deformation due to the elasticity coefficient difference between the metal and reinforcement phase. The reason fracture occurs on the LMDed Fe-Cr-B based alloy after yielding is due to the interface separation between Fe-matrix and $(Cr, Fe)_2B$ phase before sufficient plastic deformation is induced.

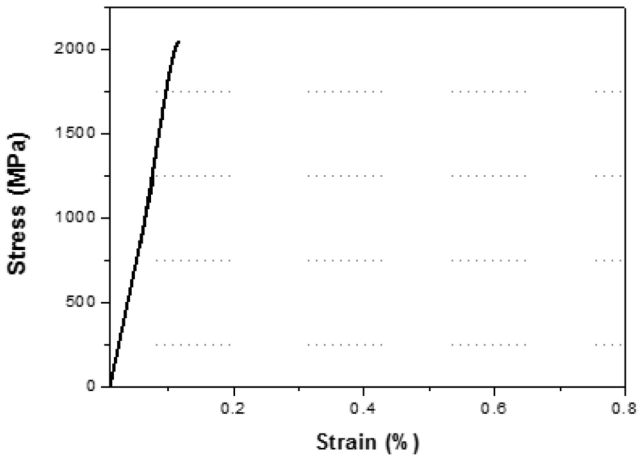


Fig. 5. Engineering compressive stress-strain curve of LMDed Fe-Cr-B alloy

Fig. 6 shows the SEM observation of the surface and cross-section of the specimen after the compression test. Macro observation (Fig. 6a) of the specimen after compression identified a main crack in the 45° direction of the specimen, and macro surface cracks other than the main crack were not observed. High magnification observation of the fracture surface confirmed that the fracture mode of the LMDed Fe-Cr-B-based alloy changed according to the boride shape. First, in the area where the needle type boride was observed in the center region of the specimen,

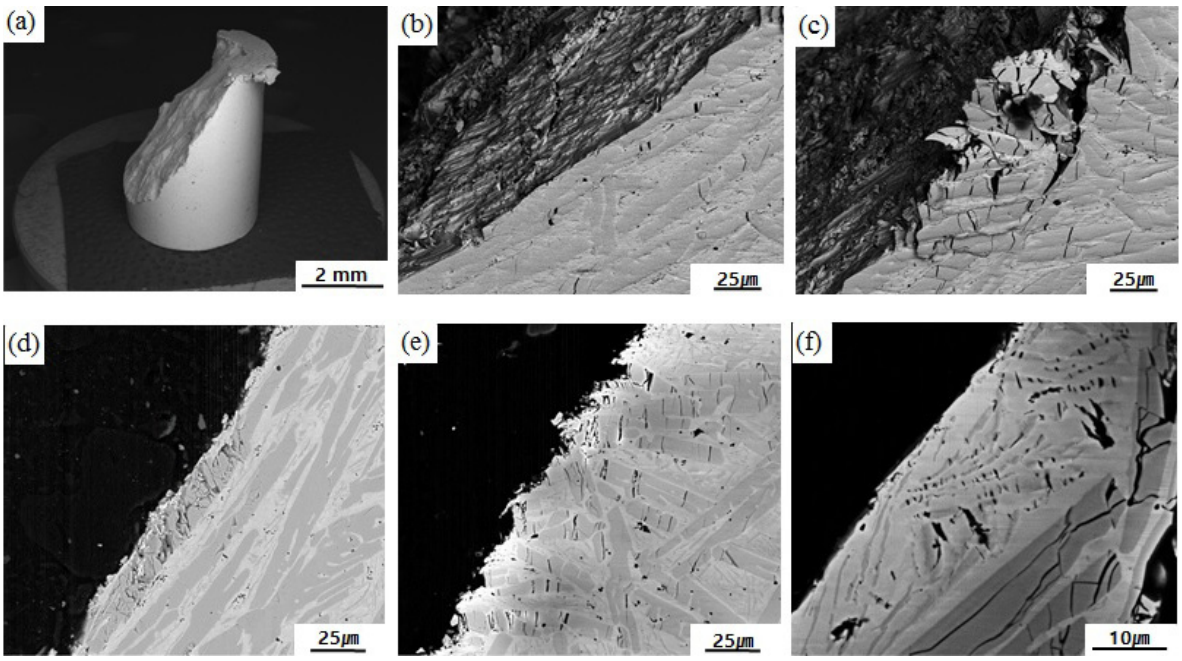


Fig. 6. SEM observation results of compressed specimen (a) macro image (b), (c) surface images and (d-f) cross-sectional images

cracks were formed along the boride distribution direction with an intergranular fracture mode (Fig. 6b). However, transgranular fracture mode was observed in the surface region where random borides were formed (Fig. 6c).

Cross-sectional observation of the fractured surface (Fig. 6d-f) was observed to make a detailed observation of the fracture modes according to boride shape, and multiple secondary cracks were formed during fracturing regardless of the boride shape. In other words, there was a difference in deformation mode according to boride shape, and fracturing occurred after yielding, but a certain adhesion level was maintained with the matrix by all boride phases, which is interpreted to be a contribution to the increased strength.

## 4. Conclusions

This study investigated the microstructural and room temperature mechanical properties of bulk type Fe-Cr-B based alloy manufactured using LMD process, and reached the following conclusions:

1. Microstructural observation confirmed that the LMDed Fe-Cr-B based alloy is an intrinsic composite in which $(Cr, Fe)_2B$ phase is evenly precipitated from the $\alpha$-Fe phase. There were two types of main boride phases, needle type and random type, and fine boride phases with 1 μm thickness were observed between the main boride phases. Phase ratio measurement confirmed Fe-matrix: 30.4%, boride: 68.3% and porosity: 1.3%.
2. As a results of evaluation of mechanical properties, the average hardness was measured as 838.4Hv. and a room temperature compression test measured peak stress of 2014.7MPa. The high hardness and super high strength of LMDed Fe-Cr-B based alloy are suspected to be achieved due to the high boride ratio and even distribution of fine boride phases.
3. The compressed specimen was observed to determine deformation and fracture behaviors, and a transgranular fracture mode was observed in the needle type boride area and an intergranular fracture mode was observed in the randomly distributed boride area. In addition, multiple secondary cracks present in all borides confirmed that the interface adhesion between the metal matrix and boride phase was maintained at a certain level regardless of boride shape.

## REFERENCES

[1] A. Rottger, J. Lentz, W. Theisen, Mater. Des. **88**, 420-429 (2015).
[2] S. Ma, J. Xing, H. Fu, Y. Gao, J. Zhang, Acta Mater. **60**, 831-843 (2012).
[3] M.F. Erinosho, E.T. Akinlabi, S. Pityana, Proceding of the world congress on engineering, (2014).
[4] C.Y. Kong, R.J. Scudamore, J. Allen, Physic. Proced. **5**, 379-386 (2010).
[5] H.J. Kim, S. Grossi, Y.G. Kweon, Met. Mater. **5**, 63 (1999).
[6] H.J Kim, B.H. Yoon, C.H. Lee, Wear **249**, 846 (2002).
[7] K.H. Lee, D.H. Nam, S.H. Lee, C.N. Paul Kim, Mater. Sci. Eng. A **428**, 124 (2006).
[8] J. Do, H.J. Lee, C. Jeon, D.J. Ha, C. Kim, B.J. Lee, S. Lee, Y.S. Shin, Metall. Mater. Trans. A 4**3A**, 2012-2237 (2012).
[9] C.Y. Son, T.S. Yoon, S. Lee, Metall. Mater. Trans. A **40A**, 1110-1117 (2009).
[10] A.A. Sorour, "Microstructure and Tribology of Fe–Cr–B-Based Alloys", Department of Mining and Materials Engineering, McGill University, Doctor of Philosophy (2014).